Flexural Analysis of Steel Fiber Reinforced Concrete Beam

강섬유 보강 콘크리트 보의 휨 해석

이 차 돈*
Lee, Cha Don

요 약

SFRC 보의 휨 거동에 대한 이론적인 해석이 제시되었다. Critical region내의 곡률 변화와 균열 양상이 고려 되었으며 이를 위해 SFRC의 압축 응력-변형도와 특히 SFRC의 인장 최대하중 후 응력-균열 열림 관계(strss-crack opening relationships)로 표현된 인장 constitutive 모델이 비선형 휨 해석에 이용되었다. 제시된 모델의 해석치는 실험치와 비교할 때 만족스러웠으며 이 모델을 이용, SFRC보의 휨 거동에 미치는 여러 영향들과 위험 단면(critical section)의 거동이 고찰되었다. 또한 단순 관찰과 통계적인 접근을 통해 SFRC 보의 휨 거동에 큰 영향을 미치는 변수(parameters)들을 찾아 내었다.

ABSTRSACT

An analytical simulation of the flexural behavior of SFRC beam has been illustrated. Curvature distributions and crack opening in critical region were taken into account. Compressive and tensile constitutive models which express post-peak behavior of SFRC with stress-crack opening relationships were incorporated in simulating nonlinear flexural behavior of the beam. The model was able to predict test results with reasonable accuracy. Behavior of the critical section and effects of different factors on the flexural behavior of SFRC beam were investigated. Simple observation and statistical approach have been made in selecting most influential parameters in flexural behavior of SFRC.

1. INTRODUCTION

The flexural behavior of SFRC is typically marked by the formation of one major crack of a critical section. This implies that more damage is done to cracked critical section and a concentration of curvature occurs in the vicinity of this section. As loading continues, the crack at the critical section begins to widen and this prompts the use of stress-crack opening relationships rather than stress-strain relationships on the tensile region of bending section. None of these features was considered in previous investigations for SFRC[1-3] although some

* 정회원, 중앙대학교 건설대학 건축공학과, 조교수

이 논문에 대한 토론은 1991년 3월 30일까지 본 학회에 보내주시면 1991년 9월호에 그 결과를 게재하겠습니다.

analytical approaches have been made in this regard for plain concretes[7].

Complete flexural load-deflection relationships, in this study are analytically constructed with crack-opening considered through conducting a flexural analysis of the critical section, and using some assumptions regarding curvature distributions in the vicinity of the critical section. Tensile and compressive constitutive models were incorporated in this analysis. The predicted flexural load-deflection relationships of SFRC reinforced with straight steel fibers are compared with experimental results, and the model is also used to conduct parametric studies on the effects of different matrix and fiber variables on the flexural performance of SFRC.

2. CONSTITUTIVE MODELS

Particular concerns are to be given in simulating peak values in strength and strain as well as ductilities in compression and tension. Fig.1 shows compressive and tensile models developed by the author for SFRC and complete characteristic expressions and empirical values for coefficients in Fig.1 can be referred to Ref.4.

3. FLEXURAL ANALYSIS

Attempts are made to consider the effects of cracking at the critical section on the release of tensile strains and the concentration of compressive strains in the vicinity of the critical section of the SFRC beam.

3.1 Curvature Distributions

Before the cracking the behavior of flexural beams can be regarded as elastic. One major opening of the crack on the tensile side will be accompanied by the relase of tensile strain and the concentration of compressive strains on the

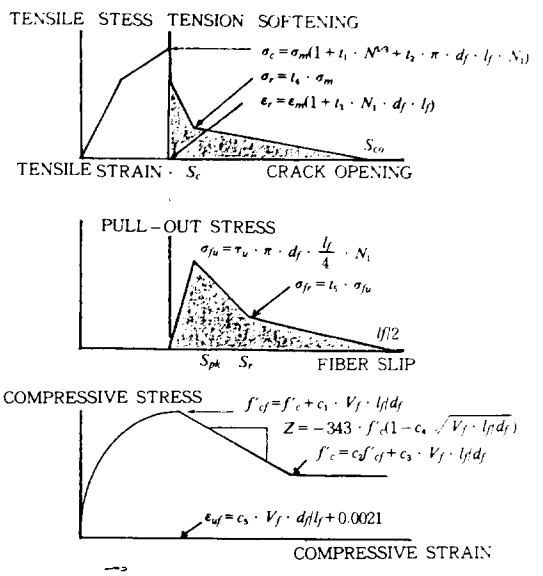

Figure 1. Constitutive Models with Material-Related and Constitutive Behavior-Related Factors
(note : Matrix softening and pull-out resistance in tensile post peak region are superimposed)

compressive side near the crack, which prevents the formation of another crack(Fig.2). A region is defined as the critical region(with a length $2 \cdot L_{cr}$ along the beam span) in which the external moment along the beam is greater than or equal to the first crack moment(M_{cr}). Outside this region the elastic beam theory is assumed to be effective. The critical region will spread outward continuously until the external load reaches its ultimate value.

After ultimate flexural load resistance starts to decrease with increasing deformations. The critical region is assumed to stabilize(in length) with curvature at this boundary assumed to stay constant at the first crack value. With constant curvatures at this boundary, deformation concentration near the center of the critical section takes the form of crack widening and increased strains in tension and compression regions, respectively.

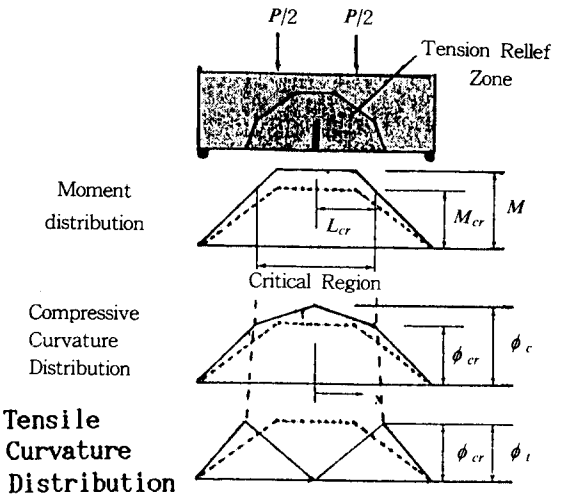

Figure 2. Moment and Curvature Distributions

3.2 Analysis of the Critical Section

The crack shape at the critical section is assumed to be linear and symmetric about a plane normal to the beam longitudinal axis. After cracking, the deformation compatibility requirements would have been disturbed if, the tensile and compressive strains were still assumed to be comparable (see Figs.3(a) and (b)). Based on deformation compatibility the crack opening angle(θ_{cr} in Fig.3(b)) can be approximated by computing the difference in rotations associated with compressive and tensile strains in the critical region(Fig.3(b)):

$$\theta_{cr}=\theta_c-\theta_t \qquad (1)$$
$$=\int_0^{L_{cr}}(\phi_c(x)-\phi_t(x))\,dx:$$

where:

θ_{cr} = crack opening angle;

$\theta_c=\int_0^{L_{cr}}\phi_c(x)\,dx$
= rotation of the compressive side of the beam at the boundary of the critical region;

$\theta_t=\int_0^{L_{cr}}\phi_t(x)\,dx$
= rotation of the tensile side of the beam at the boundary of the critical region due to tensile curvature only;

ϕ_c, ϕ_t = conpressive and tensile side curvatures, respectively; and

x = distance from center(cracked section).

The assumed linear post-cracking distributions of compressive side and tensile side curvatures in the cirtical region are:

$$\phi_c(x)=\frac{x}{L_{cr}}\cdot(\phi_c(L_{cr})-\phi_c(0)+\phi_c(0); \qquad (2)$$

$$\phi_t(x)=\frac{x}{L_{cr}}\cdot\phi_t(L_{cr}); \text{ and}$$

$\phi_c(L_{cr})=\phi_t(L_{cr})$ at the boundary of the critical region.

Incorporating the above curvatures into Eq. (1) yields crack opening angle(θ_{cr}) as well as maximum crack opening (S) at the extreme bottom layer of the critical section:

$$\theta_{cr}=0.5\cdot\phi_c(0)\cdot L_{cr}; \text{ and} \qquad (3)$$

$S=H\cdot\theta_{cr}$

where:

H = crack depth(Fig.3(b)).

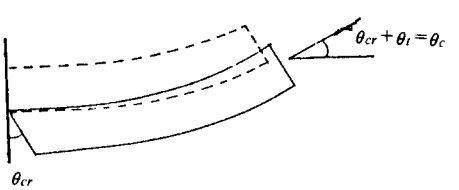

(a) Compressive Strain = Tensile Strain

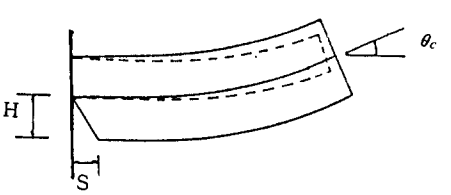

(b) Compressive Strain > Tensile Strain

Figure 3. Deformation Compatibility after Cracking

In flexural analysis an increment is made at each step in compressive side curvature at the critical section. $\phi_c(0)$, and the crack depth (H) is calculated using critical section nonlinear flexural analysis procedures(to be described later). This analysis needs input of crack opening angle (θ_{cr}) which depends on L_{cr}. The value of L_{cr}, however, can be computed after the critical section analysis is completed and the value of bending moment after curvature increment at the critical section is known. This condition requires an iterative approach in which the analysis starts with the old value of L_{cr} at the end of the previous incremental step, and it would be adjusted until there is a tolerable difference between the starting and final values of L_{cr} in an iteration cycle. Total flexural deflection (δ) is computed by adding deformations inside and outside of the critical region. Half of the beam span can be used for this purpose due to symmetry :

$$\delta = \int_0^{L_{cr}} \int_0^x \phi_c(w)\, dw dx + \int_{L_{cr}}^{L/2} \int_0^x \phi_c(w)\, dw dx \quad (4)$$

where :

L = span of the beam ;

x = distance from the critical section.

3.3 Nonlinear Flexural Analysis of the Critical (Cracked) Section

Equilibrium of axial forces at the section is satisfied through iterative selection of the neutral axis location. In order to set up the initial bracket which includes true strain configuration, the lower bound is built by assuming a strain dustribution with the given curvature but the crack depth corresponding to the previous step(Fig.4(a)). The upper bound is constructed with the curvature, assuming an extreme compressive strain equal to that at the end of the previous step(Fig.4 (b)). The iterations were conducted using a Modified Regula-Falsi method[5]. In the Modified Regula-Falsi method(Fig.5), the new side of the range within which the solution occurs is obtained as the intersection is with horizontal axis of a line connecting a point not on the function curve but at a location with ϕ ($0<\varphi\leqq 1$) times the function value. The method using φ equal to 0.5 reduced the number of iterations in finding equilibrium condition by one-half to two-thirds compared with conventional Regula--Falsi Method.

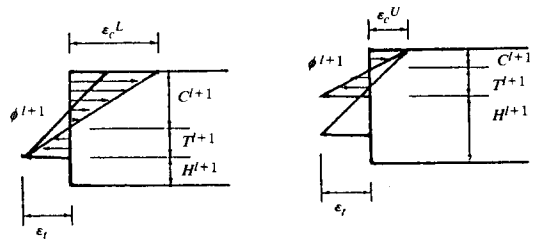

(a) Lower Bound for $(i+1)$th Step (b) Upper Bound for $(i+1)$th Step

Figure 4. Estimation of Initial Strain Configuration

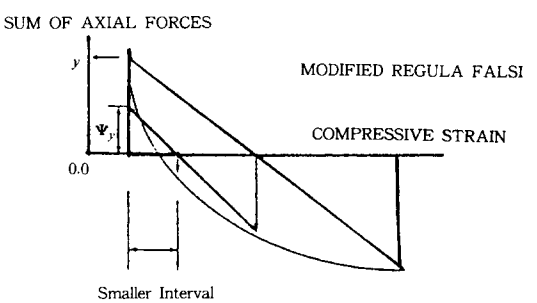

Figure 5. Modified Regula-Falsi Method

3.4 Comparison with Test Results

Comparisons between experimental and analytical flexural load-deflection curves for SFRC reinforced with straight steel fibers presented in Fig.6 are observed to be satisfactory.

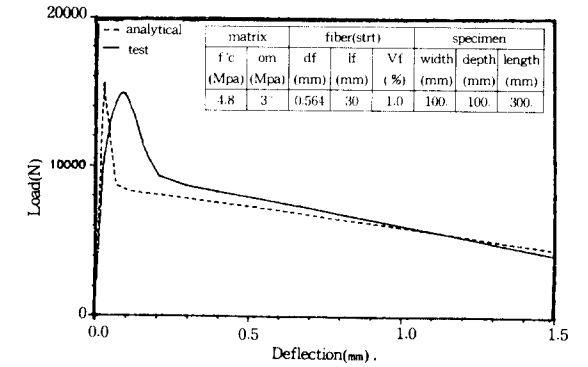

matrix		fiber(strt)			specimen		
f'c (Mpa)	om (Mpa)	df (mm)	lf (mm)	Vf (%)	width (mm)	depth (mm)	length (mm)
4.8	3	0.564	30	1.0	100.	100.	300.

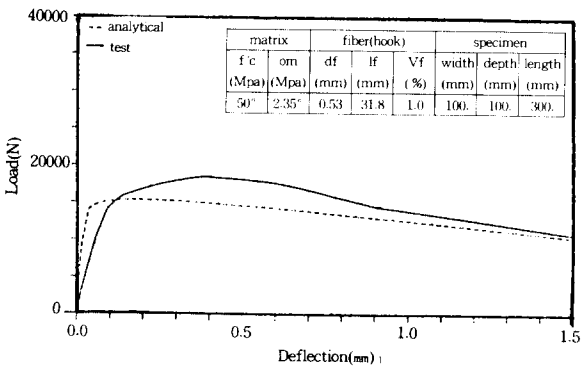

matrix		fiber(hook)			specimen		
f'c (Mpa)	om (Mpa)	df (mm)	lf (mm)	Vf (%)	width (mm)	depth (mm)	length (mm)
50	2.35	0.53	31.8	1.0	100.	100.	300.

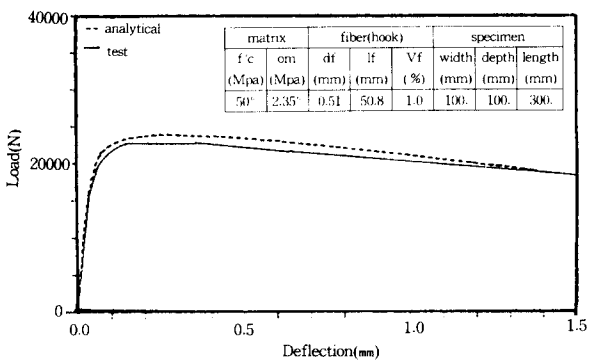

matrix		fiber(hook)			specimen		
f'c (Mpa)	om (Mpa)	df (mm)	lf (mm)	Vf (%)	width (mm)	depth (mm)	length (mm)
50	2.35	0.51	50.8	1.0	100.	100.	300.

(c)

Figure 6. Comparisions between Experimental and Analytical Flexural Load-Deflection Curves

4. FLEXURAL BEHAVIOR OF CRITICAL(CRACKED) SFRC SECTION

Figs.7(a) and (b) show the profiles of strain and stress distributions along the depth of the critical section for two different fiber volume fractions(0.5 % and 1.2 %, respectively) at the peak stresses and post-peak stresses for deflections equal to 0.5mm. In both cases the peak flexural load is attained when crack has already opened. Fig.7 shows that in the post-peak region, the post-peak tensile resistance of SFRC provided by fibers bridging the crack seems to decide performance of SFRC and also its flexural strength. This implies higher increase in flexural strength than the corresponding increase in tensile strength of SFRC. Low fiber volume fraction of 0.5 % resulted in significantly less ductility compared to high fiber volume fraction of 1.2 %, due to less tensile resistance by the fibers across the cracked section. The modulus of rupture computed using linear-elastic flexural analysis equations can actually give a characteristic stress value which relates to the peak tensile strength of SFRC.

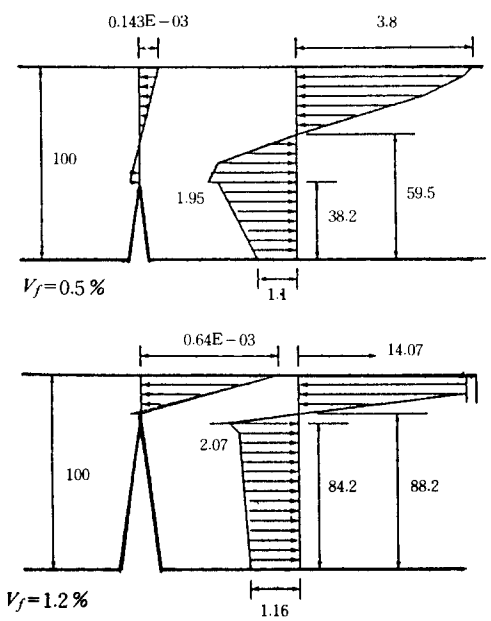

(a) Strain and Stress Distributions at Peak Load

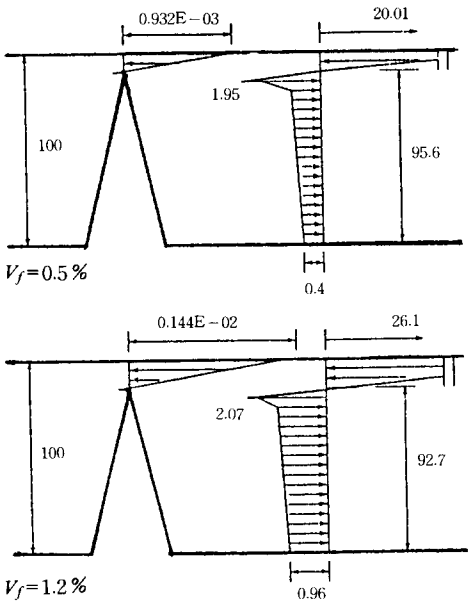

(b) Strain and Stress Distributions at Deflection equal to 0.5mm

Figure 7. Strain and Stress Distrubutions at the Critical Section

5. A PARAMETRIC STUDY ON SFRC FLEXURAL BEHAVIOR

The parametric study consists of analytically investigating the effects of changing the values from "standard" ones chosen either on the basis of test results or considering practical ranges applicable to SFRC(see Table 1 and 2) on flexural behavior of SFRC. Two groups of factors were considered in this study : ten material-related factors and ten constitutive bahavior-related facotrs(see Fig.1, Table 1 and 2). The effects of variations in twenty different factors on the flexural peak load(P), ductility(D), toughness(A), and overall flexural behavior of SFRC beams (V) were investigated analytically(see Fig.8). Here, the overall flexural behavior was measured as :

$$v=\sum_{i=1}^{i=3}\gamma_i \cdot v_i^2 \qquad (5)$$

where :

γ_i = weighing coefficients for each factor ;

$v_1=\dfrac{P_v-P_s}{P_s}$;

$v_2=\dfrac{D_v-D_s}{D_s}$;

$v_3=\dfrac{A_v-A_s}{A_s}$;

P = peak flexural load(Fig.8) ;

D = ductility

$= P/P_r$(see Fig.8) ; and

A = toughness

= area under load-deflection curve as defined in Fig.8.

Considering the fact that γ_1, γ_2 and γ_3 explain discrepancies in pre-peak behavior, behavior between pre-peak and post-peak, and post--peak behavior, equal weights(weighing coefficients equal to 1.0) are given to each of these factors.

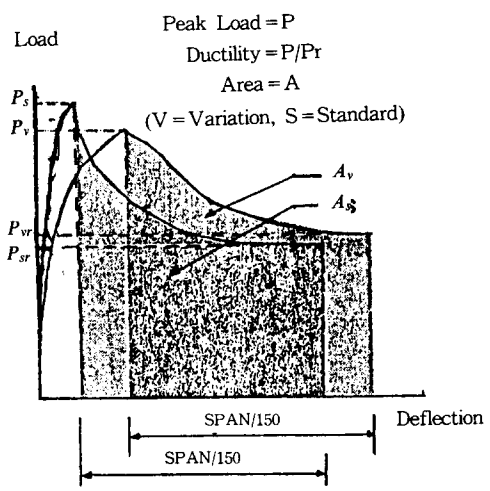

Figure 8. Definitions of Four Different Criteria

Conclusions regarding the significance of the effects of different factors on SFRC flexural

behavior have been based on simple observations as well as statistical analysis based on 2^k factorial designs[6]. For simple observations, only one of the factors is varied in each run and corresponding varitations in the four aspects of flexural behavior were assessed analytically using the flexural analysis procedures developed in this investigation. Then these values are further normalized with respect to the values corresponding to the "standard" condition. The minimum and maximum values of each material-related factors and the constitutive behavior-related factors were equal to 0.5 and 2.5, and 0.5 and 1.5 times the corresponding "standard" values, respectively, which would represent limit values in practical conditions commonly encountered in SFRC.

The results are shown in Table 1 for material-related factors and in Table 2 for constitutive behavior-related factors(note that a larger number is indicative of a larger effect).

Table 1. Effects of Material-Related Factors

Factors	Standard Value	Variation	Maximum Normalized Differences			
			Peak Load	Ductility	Tough-ness	Overall Behavior
σ_m	3	2-4	0.298	0.438	0.014	0.274
f'_c	40	30-50	0.045	0.023	0.015	0.002
S_{cr}	0.008	0.003-0.02	0.199	0.076	0.064	0.049
S_0	0.023	0.01-0.05	0.0	0.036	0.006	0.001
d_f	0.5	0.25-1.00	0.151	0.697	0.891	0.457
l_f	0.30	20-40	0.025	0.361	0.361	0.264
V_f	0.01	0.005-0.02	0.042	0.475	0.52	0.457
τ_u	2.62	1.0-4.5	0.02	0.68	0.689	0.939
S_{pk}	0.025	0.01-0.05	0.031	0.015	0.011	0.001
S_r	2.8	1.0-5.0	0.0	0.531	0.322	0.32

* Maximum Normalized Difference = Maximum absolute difference in a certain aspect of flexural bahavior divided by "Standard Value" of that aspect due to changes in certain factor.

5.1 Influence of Matrix Strength

Fig.9(a) shows that matrix tensile strength (σ_m) has little influence on flexural toughness

Table 2. Effects of Constitutive Behavior Related Factors

Factors	Standard Value	Variation	Maximum Normalized Differences			
			Peak Load	Ductility	Tough-ness	Overall Behavior
t1	0.138	0.069-0.207	0.001	0.004	0.002	0.0
t2	0.050	0.025-0.075	0.001	0.004	0.002	0.0
t3	0.35	0.175-0.525	0.023	0.059	0.021	0.004
t4	0.40	0.2-0.6	0.067	0.028	0.027	0.006
t5	0.3	0.15-0.45	0.0	0.291	0.097	0.016
c1	3.6	1.8-5.4	0.006	0.023	0.01	0.0
c2	0.12	0.06-0.18	0.0	0.0	0.0	0.0
c3	14.8	7.4-22.2	0.0	0.0	0.0	0.0
c4	0.66	0.33-0.99	0.0	0.0	0.0	0.0
c5	0.0007	0.0004-0.002	0.019	0.034	0.008	0.0

* Maximum Normalized Difference = Maximum absolute difference in a certain aspect of flexural bahavior divided by "Standard Value" of that aspect due to changes in certain factor.

of SFRC bacause the peak flexural strength of SFRC usually occurs with crack opened and penetrated into the critical section in which the pull-out action of fibers bridging the crack plays important role. Compressive strength of plain concrete (f'_c) has very little influence on the flexural bahavior of SFRC bacause pre-peak compressive constitutive bahavior of SFRC can only be partly utilized under flexure due to the weak tensile strength of steel fiber reinforced concrete.

5.2 Influence of Matrix Softening in Tension

Fig.9(b) shows that the increase in crack opening at residual matrix tensile strength (S_{cr}) increases only the flexural strength and tougness of SFRC to some extent.

5.3 Influences of Fiber Dimensions and Fiber Volume Fraction

As the fiber diameter decreases, the peak flexural strength, ductility and toughness of SFRC increase, which may be attributed to the increase in the number of fibers per unit corss-sectional area and the available fiber-to-matrix interfacial bond area. The increase in fiber length (Fig.10), influences ductility and toughness but to a relatively small extent the flexural strength

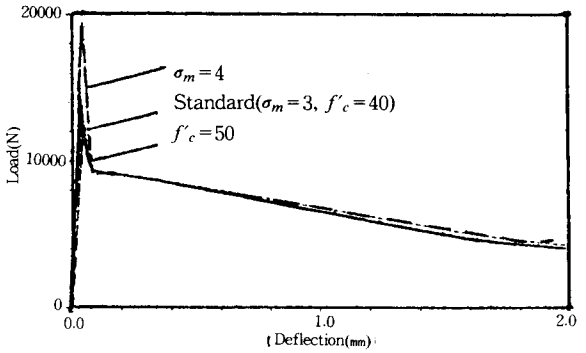

(a) Influence of Matrix Strength

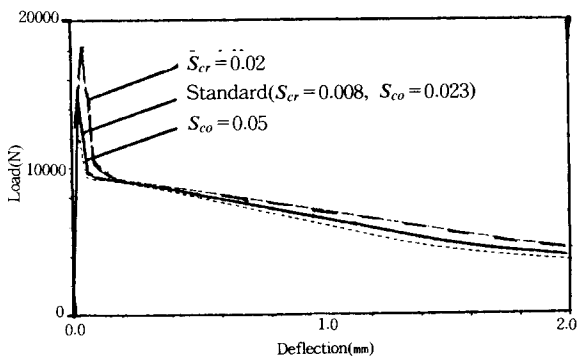

(b) Influence of Matrix Softening in Tension

Figure 9. Influence of Matrix on Load-Deflection Curve

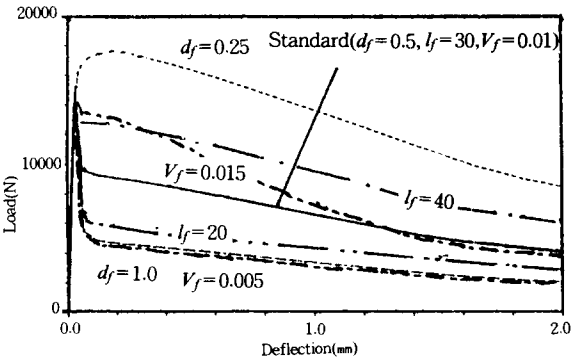

Figure 10. Influences of Fiber Dimensions and Fiber Volume Fractions

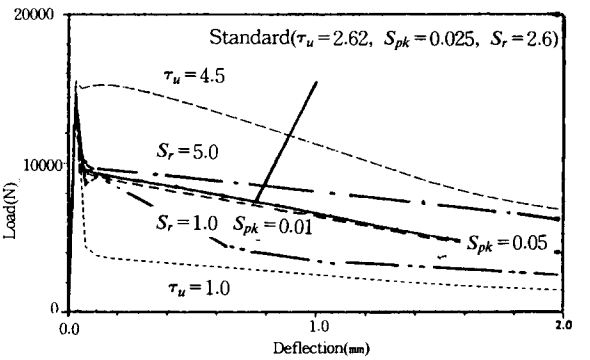

Figure 11. Influence of Fiber of Fiber Pull-Out Behavior

of SFRC due to reduced number of fibers crossing unit cross-sectional area. The increase(decrease) in fiber volume fraction increases(decreases) the flexural ductility and toughness, and to some extent the flexural strength of SFRC (Fig.10). This factor is observed to have important effects on flexural behavior.

5.4 Influence of Fiber Pull-Out Behavior

Fig.11 shows that as the bond strength(τ_u) increases(decrases), the flexural ductility and toughness of SFRC tend to increase(decrease) significantly. Slip at peak fiber pull-out strength (S_{pk}) is observed in Fig.11 to have negligible effects on flexural behavior. This suggests that pull-out stiffness is not an important factor in deciding the flexural behavior of SFRC. Fig.11 also shows that fiber slip at residual pull-out strength(S_r) has relatively important effects on flexural ductility and toughness, but not on flexural strength of SFRC.

5.5. Influence of Constitutive Behavior-Related Factors

Table 2 illustrates much smaller effect of these factors when compared with those resulting from variations in influential material-related factors(which typically result in 70% to 80% variations in flexural performance characteristics).

Table 3 summarizes the results of analyses

based on 2^k factorial design for the influence of material-related factors on flexural behavior in which factors corresponding to higher numerical values are more influential than others in deciding a specific aspect of flexural behavior.

Table 4 summarizes the results of Table 1 and 3. It is interesting to note that generally similar results are obtained both for the 2^k factorial design and the simple observation of flexural load-deflection curves.

Table 3. Effects of Material-Related Factors (2^k Factorial Design)

Factors	f · Values on Different Criteria(x 1000)			
	Peak Load	Ductility	Toughness	Overall Behavior
σ_m	1349	38	20712	20.14
f'_c	22	0.32	249	0.19
S_{cr}	183	1.69	1889	0.08
S_0	0.71	0.0	489	0.02
d_f	383	161	706830	77
l_f	147	51	244490	34.4
V_f	244	91	425800	54.19
τ_u	343	231	865120	84
S_{pk}	18	0.33	662	0.087
S_r	2.4	145	195130	60

Table 4. Effects of Material-Related Factors in Order

Criteria	Factors	Order					
		1	2	3	4	5	6
Peak Load	S.O*	σ_m	d_f	S_{cr}	V_f	.....	.....
	$2 \cdot k$	σ_m	d_f	τ_u	V_f	S_r	l_f
Ductility	S.O.	τ_u	S_r	d_f	l_f	V_f	σ_m
	$2 \cdot k$	τ_u	d_f	S_r	V_f	l_f	σ_m
Toughness	S.O.	d_f	τ_u	V_f	l_f	S_r	.....
	$2 \cdot k$	τ_u	d_f	V_f	l_f	S_r	σ_m
Overall Behavior	S.O.	τ_u	d_f	V_f	S_r	σ_m	l_f
	$2 \cdot k$	τ_u	d_f	S_r	V_f	l_f	σ_m

* Most important factor based on the "Simple Observation" of flexural load-deflection relationships.

6. CONCLUSION

Strong dependence of flexural strength of SFRC on its post-peak tensile behavior and the higher increases in flexural strength than the corresponding increase in tensile strength for given fiber reinforcement conditions are observed. Calculation of modulus of rupture based on linear-elastic flexural analysis equations can not thus provide with a characteristic stress value which directly relates to the peak tensile strength of SFRC.

The results of parametric study indicated that : (1) The flexural strength of SFRC was most sensitive to the variation in matrix tensile strength ; (2) Ductility(D), toughness(A) and overall flexural behavior(V) are most influenced by fiber diameter and fiber pull-out strength ; (3) Matrix compressive strength, crack opening at which matrix tensile stress diminishes, and fiber slip at peak pull-out load have negligible effects on flexural behavior of SFRC ; (4) Fiber dimensions(fiber diameter and fiber length) as well as fiber volume fraction have almost equally important effects on flexural behavior ; (5) While the matrix crack opening at residual matrix tensile strength has little effects on different aspects of flexural behavior, fiber slip at residual pull-out strength has relatively important effect on flexural ductility and overall flexural behavior of SFRC ; (6) Fiber-to-matrix bond strength (τ_u), fiber dimensions and volume fraction(d_f, l_f and V_f), matrix tensile strength(σ_m) and slip at residual pull-out strength(S_r) are the most influential factors deciding the flexural behavior of SFRC ; and (7) Similar observations were made by analysis using 2^k factorial design and also through simple observation of flexural load-deflection curves.

REFERENCES

(1) Sakai, M. and Nakamura, N., "Analysis of Flexural Behavior of Steel Fiber Reinforced Concrete," Rilem, 1986.

(2) Babut, R. and Brandt, A.M., "The Method of Testing and Analyzing of Steel Fibre Reinforced Concrete Elements in Flexure," RILEM, 1978, pp.479－486.

(3) Rafagopalan, K. Parameswaran V.S. and Ramaswamy, G.S., "Strength of Steel Fiber Reinforced Concrete Beams," Indian Concrete Journal, January 1974, pp.17－25.

(4) Soroushian, P. and Lee, C.D., "Constitutive Modeling of Steel Fiber Reinforced Concrete Under Tension and Compression," Symposium for Steel Fiber Reinforced Concrete, London, United Kingdom, September 1989.

(5) Conte, S,D. and de Boor, C., "Elementary Numerical Analysis," McGraw－Hill Co., Reading, 1980.

(6) Walpole, R.E. and Myer, R.H., "Probability and Statistics for Engineers and Scientists," McMillan Publishing Co., Reading, 1978.

(7) Hillerborg, A., "Numerical Methods to Simulate Softening and Fracture of Concrete," Fracture Mechanics of Concrete : Structural Application and Numerical Calculation, Martinus Nijhoff Publishers, 1985.

(접수일자 : 1990. 8. 7)